4-6-2022

Sex Differences in the Fecal Microbiome and Hippocampal Glial Morphology Following Diet and Antibiotic Treatment

Anju Saxena

Roberta R M Moran

Meghan R. Bullard

Emma O. Bondy

Matthew Foster Smith

See next page for additional authors

Authors

Anju Saxena, Roberta R M Moran, Meghan R. Bullard, Emma O. Bondy, Matthew Foster Smith, Lainie Morris, Nicaella Fogle, Jagroop Singh, Brendan Jarvis, Tammy Ray, Juhi Saxena, and Linnea Ruth Freeman

RESEARCH ARTICLE

Sex differences in the fecal microbiome and hippocampal glial morphology following diet and antibiotic treatment

Anju Saxena[1], Roberta R. M. Moran[1], Meghan R. Bullard[2], Emma O. Bondy[1], Matthew Foster Smith[1], Lainie Morris[2], Nicaella Fogle[1], Jagroop Singh[2], Brendan Jarvis[1], Tammy Ray[1], Juhi Saxena[1], Linnea Ruth Freeman[1,2]*

1 Neurosciences, Furman University, Greenville, South Carolina, United States of America, 2 Department of Biology, Furman University, Greenville, South Carolina, United States of America

* linnea.freeman@furman.edu

Abstract

Rising obesity rates have become a major public health concern within the United States. Understanding the systemic and neural effects of obesity is crucial in designing preventive and therapeutic measures. In previous studies, administration of a high fat diet has induced significant weight gain for mouse models of obesity. Interestingly, sex differences in high-fat diet-induced weight gain have been observed, with female mice gaining significantly less weight compared to male mice on the same high-fat diet. It has also been observed that consumption of a high-fat diet can increase neurogliosis, but the mechanism by which this occurs is still not fully understood. Recent research has suggested that the gut microbiome may mediate diet-induced glial activation. The current study aimed to (1) analyze changes to the gut microbiome following consumption of a high fat (HF) diet as well as antibiotic treatment, (2) evaluate hippocampal microgliosis and astrogliosis, and (3) identify sex differences within these responses. We administered a low fat (Research Diets D12450 K) or high fat diet (Research Diets D12451) to male and female C57Bl/6 mice for sixteen weeks. Mice received an antibiotic cocktail containing 0.5g/L of vancomycin, 1.0 g/L ampicillin, 1.0 g/L neomycin, and 1.0 g/L metronidazole in their drinking water during the last six weeks of the study and were compared to control mice receiving normal drinking water throughout the study. We observed a significant reduction in gut microbiome diversity for groups that received the antibiotic cocktail, as determined by Illumina next-generation sequencing. Male mice fed the HF diet (± antibiotics) had significantly greater body weights compared to all other groups. And, female mice fed the low fat (LF) diet and administered antibiotics revealed significantly decreased microgliosis and astrogliosis in the hippocampus compared to LF-fed females without antibiotics. Interestingly, male mice fed the LF diet and administered antibiotics revealed significantly increased microgliosis, but decreased astrogliosis, compared to LF-fed males without antibiotics. The observed sex differences in LF-fed mice given antibiotics brings forward questions about sex differences in nutrient metabolism, gut microbiome composition, and response to antibiotics.

Introduction

Rising obesity rates have become a major public health concern within the United States. By 2030, the obesity prevalence in the United States is expected to rise to an alarming 46–47% [1]. Obesity rates in 1999–2000 were 30.9% for US adults [2] and 42.4% in 2017–2018 [3], indicating the considerable rise in obesity prevalence during the last twenty years. Understanding the systemic and neural effects of obesity is crucial in designing preventive and therapeutic measures.

Obesity is a complex metabolic disease characterized by excessive weight gain and a body mass index greater than 30 kg/m2 [4]. Co-morbidities such as diabetes, cancer, and cardiovascular disease lead to increased mortality [5, 6]. Consumption of a Western Diet is a contributing factor to the rising obesity rates. The Western Diet refers to a high fat diet consisting of high levels of saturated fats and simple sugars [7, 8].

In previous studies, administration of a high fat diet has induced significant weight gain for mouse models of obesity [8–11]. Interestingly, sex differences in high fat diet-induced weight gain have been observed; female mice gain significantly less weight compared to male mice on the same high fat diet [10, 12]. These sex differences extend to adipose tissue inflammation, hyperinsulinemia, and islet hypertrophy, with female mice demonstrating a resistance to these conditions compared to male mice [13]. While estrogen, cytokine, and gut metabolite levels have all been implicated as potential mediators of these observed sex differences, the mechanism by which these sex differences arise is still not well understood [13–16].

In addition to weight gain, consumption of a high fat diet alters gut microbiome composition [8, 16]. The gut microbiome refers to the microorganisms, and their genetic material, that reside within the gut. In response to a high-fat diet, the gut microbiome undergoes compositional changes that can decrease the diversity of bacteria and thereby induce gut dysbiosis [9, 17]. High fat diets have been shown to change the bacterial levels of the two most abundant phyla of bacteria within the gut, increasing Firmicutes and decreasing Bacteroidetes [5, 18, 19]. Changes within these bacterial phyla can also alter levels of bacterial metabolites such as lipopolysaccharides and short-chain fatty acids (SCFAs), which contribute to systemic effects of obesity [20–23].

Furthermore, high fat diet consumption can activate and alter the morphology and function of glial cells within the brain, including microglia and astrocytes [9, 11, 24–27]. Microglial cells are the resident immune cells of the brain and exhibit changes in number and activation state in response to inflammatory events [28, 29]. Astrocytes have a number of roles in the brain, including metabolic, immune, and vascular support; they are the most abundant glial cell in the brain [11, 30, 31]. The hippocampus, a brain region involved in learning and memory, is vulnerable to obesity-induced inflammation. High saturated fat and refined sugar intake, characteristic of the Western Diet, are linked to deficits in hippocampal-dependent learning and memory in adults [32, 33]. For example, obese mice perform significantly worse than controls on tasks that require hippocampal cognitive function [34–36]. Cognitive impairment in diet-induced obesity is associated with increased microglial activation [37]. An increase in activated microglia has been reported in the hippocampus of mice fed a high fat diet [38, 39] and a high fat, high sugar diet [9].

While it has already been established that consumption of a high fat diet can induce glial activation, the mechanism by which this occurs is still not fully understood. Recent research has suggested that the gut microbiome may mediate this effect [17]. Consumption of a high fat diet can induce compositional changes within the gut microbiome and these compositional changes could drive the neuroinflammatory response within the brain. There is a growing

body of evidence that suggests the gut microbiome and its metabolites may mediate the neuroinflammatory response to a high-fat diet.

In order to investigate the role of gut microbiome diversity on hippocampal microglia morphology, we included administration of an antibiotic cocktail in the drinking water to significantly deplete gut microbiome diversity and test its effects. Specifically, we measured the fecal microbiome as an indicator of changes occurring at the level of the gut microbiome. We included the antibiotics vancomycin, ampicillin, neomycin, and metronidazole as has been previously performed in mice and resulted in microbiota depletion [40–42]. The current study aimed to (1) analyze changes to the gut microbiome following consumption of a high fat (HF) diet as well as antibiotic treatment, (2) evaluate hippocampal microgliosis and astrogliosis, and (3) identify sex differences within these responses. Given previous results that have shown sex differences in high fat diet-induced obesity, gut microbiome composition, as well as neurogliosis, we designed this study in order to evaluate each of these components. The antibiotic cocktail was administered in order to significantly deplete gut microbiome composition and diversity and therefore, test the effects when this variable was altered. We hypothesized that severely depleting gut microbiome diversity in both sexes would normalize differences in neurogliosis. If sex differences in the gut microbiome are a factor for sex differences in neurogliosis, then significantly depleting gut microbiome diversity in both sexes should lead to similar changes to neuroglia.

Materials and methods

Animals, diets, and treatments

Sixty-five C57B1/6 mice (The Jackson Laboratory, Bar Harbor, ME, USA) were housed 2–4 to a cage under a controlled, 12-hour light/ 12-hour dark cycle with *ad libitum* access to food and water. Mice were received at 6 weeks and were allowed to acclimate to the vivarium for 2 weeks. Two-month-old male (n = 32) and female (n = 33) mice were randomly assigned to the following diet groups: High Fat (HF) (n = 33) and Low Fat (LF) (n = 32). Mice were then further divided into antibiotic groups: antibiotic drinking water (n = 35) and normal drinking water (n = 30). This created a total of eight experimental groups: Male LF (n = 6), Male LF Antibiotics (n = 9), Male HF (n = 7), Male HF Antibiotics (n = 10), Female LF (n = 9), Female LF Antibiotics (n = 8), Female HF (n = 8), and Female HF Antibiotics (n = 8).

The LF control diet consisted of (by calorie): 20% protein, 70% carbohydrate, and 10% fat (D12450 K; Research Diets Inc. New Brunswick, NJ, USA). The HF treatment diet consisted of (by calorie): 20% protein, 35% carbohydrate, and 45% fat (D12451; Research Diets Inc., New Brunswick, NJ, USA). Soybean oil and lard were the primary sources of fat for these diets. Both diets had the same amount of vitamin and mineral content. The antibiotic cocktail was administered through the drinking water and consisted of 0.5g/L of vancomycin, 1.0 g/L ampicillin, 1.0 g/L neomycin, and 1.0 g/L metronidazole (Cayman Chemical, Ann Arbor, MI, USA). The diets were administered for 16 weeks. Antibiotics were added to the drinking water during the last 6 weeks of the total 16-week study. Throughout the 16-week study, body weight and food consumption were evaluated weekly by manually weighing the mice and the food remaining in the home cage. Caloric consumption was calculated by multiplying the food consumption for the cage for the LF diet by 3.82 kcals/g and 4.7 kcals/g for the HF diet. These values were further divided by the number of animals in the cage to determine the estimated caloric consumption for individual animals. This was done in order to compare caloric consumption across cages with varying numbers of animals (2-4/cage); it was not intended to obtain accurate individual consumption. Animal protocols were approved by the Furman University Animal Care and Use Committee; we received written consent for the protocol

(Approval Number 13-18-02). Our protocols were carried out according to the guidelines from the National Institute of Health.

Microbiome analyses

Fecal samples were collected using sterile technique on the last day of the study (after 16 weeks of diet administration, at the time of euthanization) and stored in microcentrifuge tubes at -80°C until analysis. Genomic DNA was isolated from fecal samples using the PowerSoil® DNA Isolation Kit (Qiagen) following the manufacturer's instructions. As an alternative to the recommended 250mg of soil, approximately 200mg of fecal sample was added to the Power-Beads tube to undergo cell lysis. The purified DNA was eluted from the spin filter using 50uL of solution C6 and stored at -20°C until PCR amplification. The 16S universal Eubacterial primers 515F GTGCCAGCMGCCGCGGTAA and 806R GGACTACVSGGGTATCTAAT were utilized to evaluate the microbial ecology of each sample on the HiSeq 2500 with methods via the bTEFAP® DNA analysis service. Each sample underwent a single-step 30 cycle PCR using HotStarTaq Plus Master Mix Kit (Qiagen, Valencia, CA, USA) and were used under the following conditions: 94°C for 3 minutes, followed by 30 cycles of 94°C for 30 seconds; 53°C for 40 seconds and 72°C for 1 minute; after which a final elongation step at 72°C for 5 minutes was performed. Following PCR, all amplicon products from different samples were mixed in equal concentrations and purified using Agencourt Ampure beads (Agencourt Bioscience Corporation, MA, USA). Samples were sequenced utilizing the Illumina MiSeq chemistry following manufacturer's protocols.

The Q25 sequence data derived from the sequencing process was processed using a proprietary analysis pipeline (www.mrdnalab.com, MR DNA, Shallowater, TX). Sequences were depleted of barcodes and primers, then short sequences < 200bp were removed; sequences with ambiguous base calls were removed, and sequences with homopolymer runs exceeding 6bp removed. Sequences were then denoised and chimeras removed. Operational taxonomic units were defined after removal of singleton sequences, and clustering at 3% divergence (97% similarity) [43–46]. OTUs were then taxonomically classified using BLASTn against a curated NCBI database and compiled into each taxonomic level.

Alpha and beta diversity analysis was conducted as described previously [43–46] using Qiime 2 [47]. Significance reported for any analysis is defined as p<0.05.

Tissue collection and immunohistochemistry

Mice were anesthetized deeply with isoflurane gas and then decapitated. Brain collection was conducted immediately following decapitation. The right hemisphere of the brain was drop-fixed with 4% paraformaldehyde for 48 hours, and then cryoprotected in 30% sucrose in 0.1 M phosphate buffered saline at 4°C. Coronal sections (40 μm) through the dorsal hippocampus were collected using a cryostat (Microm HM 505e). Sections were then processed using standard immunohistochemistry procedures as described by previously published protocols [9, 48]. Every 6th brain section through the dorsal hippocampus was evaluated. First, sections were incubated with ionized calcium binding adaptor protein (Iba-1, 1:1,000, FUJIFILM Wako, Osaka, Japan) or glial fibrillary acidic protein (GFAP; 1:1,000, Abcam, Cambridge, MA, USA) at 4°C overnight. After primary antibody incubation, the tissue was washed in phosphate buffered saline with Triton X-100 (detergent) and then incubated in biotinylated goat anti-rabbit secondary antibody (1:500, Jackson ImmunoResearch, West Grove, PA, USA) for 2 hours at room temperature. Sections were washed and placed in Elite ABC reagent (Vector Laboratories, Burlingame, CA, USA) for 1.5 hours. The tissue was developed using a Vector VIP Kit (Vector Laboratories, Burlingame, CA, USA). Finally, sections were washed, mounted, and

coverslipped on slides with Vectamount (Vector Laboratories, Burlingame, CA, USA). Slides were then analyzed and photographed using a light microscope.

Analysis of microglial cells

Microglial cells rapidly change morphology in response to immune challenges in the local environment; they can change states between ramified/resting to activated and phagocytic/amoeboid. The changes occur along a spectrum rather than a binary switch [28]. Therefore, characterizing features of microglia using FracLac and Skeleton analyses allows for comparisons between groups [29, 49]. Overall, resting microglial cells are characterized by long processes and extensive branching while activated microglial cells have a dense cell body and minimal branching [28, 50]. To evaluate these states, microglia in the hippocampus were evaluated based on branch length plus endpoints (FracLac), density, span ratio (cell shape), circularity, fractal dimension (cell complexity), and endpoints (branch number). Microglia were imaged at 100x and processed using ImageJ (National Institute of Health, https://imagej.nih.gov/ij/). Both the Analyze Skeleton Plugin (http://imagej.net/AnalyzeSkeleton31) and the FracLac for ImageJ Plugin (http://rsb.info.nih.gov/ij/plugins/frac-lac.html) were used to analyze the microglial cells, as performed previously [9, 29, 49]. The Analyze Skeleton Plugin allowed for the determination of the number of summed microglial endpoints per soma and the number of summed microglial branch lengths per soma. Six to seven images, each containing at least one microglial cell, from each animal (3–5 per group), were captured in the dorsal hippocampus. The researcher capturing images was blind to the groups. A different researcher, also blind to the groups, performed ImageJ analyses. Each image had the FFT Bandpass filter applied to the image, the brightness adjusted, and the unsharp mask and despeckle tools were also used to refine the image before thresholding. After thresholding the image, it was again despeckled, made binary, and the outliers were removed. The background noise of the image around the microglial cell was then cleared manually by the researcher. The image was then converted to a skeleton form using the Analyze Skeleton Plugin and skeletonize features. This allowed for the collection of tag skeleton features that were relevant to determining the microglial activation state: slab voxels (branch length) and endpoints. Values for branch length less than 1.75 mm were removed and the FracLac Plugin was used to determine: endpoint plus branch length, cell complexity (fractal dimension), density, circularity, and cell shape (span ratio).

Analysis of astrocytes

Microscopy images were captured at 10x and then processed using ImageJ (National Institute of Health, https://imagej.nih.gov/ij/). With ImageJ, a threshold was applied and then the percentage of area covered by astrocytes in each image was calculated, as performed previously [9]. 3–4 images per mouse were analyzed from 4–5 animals per treatment group. Data were analyzed by two different researchers, blind to the groups, and their results were averaged.

Statistical analysis

All statistical tests were conducted using GraphPad Prism (GraphPad Software, La Jolla, California, USA, www. graphpad.com). For food consumption, a mixed-effects analysis (sex x treatment x time) was performed due to a few missing values (researcher error). Body weights were log transformed and then analyzed using a three-way ANOVA (sex x treatment x time). And, a two-way (sex x treatment) ANOVA was used to determine significant differences in microglia and astrocyte measurements (data were normally distributed according to the Shapiro-Wilk test). A Tukey's posthoc analysis was conducted for any measures that indicated

statistically significant differences for the ANOVA. Fecal microbiome results were analyzed using a Kruskal–Wallis test followed by a two-stage linear step-up procedure of Benjamini, Krieger, and Yekutieli in order to control for multiple comparisons by controlling the false discovery rate. Fecal microbiome data were analyzed for all eight groups, and a separate analysis excluding the antibiotic-treated groups was also conducted in order to evaluate sex and diet effects, alone.

Results

Food consumption and body weights

A significant effect of time (F(3.320, 184.4) = 86.86; p <0.0001), a significant effect of treatment (F(7, 57) = 47.99; p <0.0001), and a significant interaction effect for time and treatment (F(105, 833) = 5.959; p <0.0001) were observed for caloric consumption over the whole study period (data not shown). Significant differences between average caloric consumption for the whole study were determined between Male LF and Female LF (p = 0.0018), Male LF and Male LF Antibiotics (p<0.0001), Male LF Antibiotics and Male HF Antibiotics (p<0.0001), Female LF Antibiotics and Female HF Antibiotics (p<0.0001), Female HF and Female HF Antibiotics (p = 0.0023), Male HF Antibiotics and Female HF Antibiotics (p<0.0001) (Fig 1A).

There was a significant effect of treatment (F(3, 57) = 14.39; p<0.0001) and a significant effect of sex (F(1, 57) = 15.76; p = 0.0002) on body weight gain (Fig 1B). There was also a significant interaction effect between sex and treatment (F(3, 57) = 5.822; p = 0.0015) on body weight gain. Specifically, Male HF gained significantly more weight than Male LF (p = 0.0005). Additionally, Male HF gained significantly more weight than Female HF (p = 0.0032), demonstrating sex differences in weight gain. Male HF Antibiotics gained significantly more weight than Female HF Antibiotics (p = 0.0052) and Male LF Antibiotics (p = 0.0004).

Microbiome analyses

After stringent quality sequence curation, a total of 2,656,509 sequences were parsed and 2,534,448 were then clustered. 2,486,339 sequences identified within the Bacteria and Archaea domains were utilized for final microbiota analyses. The average reads per sample was 51,798. For alpha and beta diversity analysis, samples were rarefied to 20,000 sequences.

We determined a significant reduction in diversity indices (Shannon Diversity; Fig 2A, Operational Taxonomic Unit; Fig 2B, Faith's Phylogenetic Diversity; Fig 2C) due to antibiotic treatment, with some variation due to diet and/or sex. Interestingly, Female LF Antibiotics revealed an increased Shannon Diversity index compared to all other antibiotic-treated groups (compared to Male LF Antibiotics, p = 0.0096; compared to Female HF Antibiotics, p = 0.0248; compared to Male HF Antibiotics, p = 0.0131; Fig 2A).

The principal coordinate (PCoA) plot of weighted UniFrac data further displays differences between antibiotic and normal drinking water groups (Fig 3). Interestingly, Male LF Antibiotics (pink), Male HF Antibiotics (yellow) and Female HF Antibiotics (blue) reveal very similar results between animals, within their groups. On the other hand, Female LF Antibiotics (green) reveals greater variance in results between animals, which is also found for normal drinking water groups. The double dendrogram (Fig 4) revealed a significant effect of antibiotic treatment on gut microbiome diversity. Furthermore, there is some additional clustering based on diet.

Fecal microbiome genera abundances revealed differences due to sex, diet, and/or antibiotic treatment (Fig 5). For male and female mice fed the LF and HF diet, antibiotics significantly depleted most genera of bacteria. *Lactococcus* was the dominant genus of bacteria for antibiotic-treated groups.

A. Average Food Consumption

B. Body Weight Gain
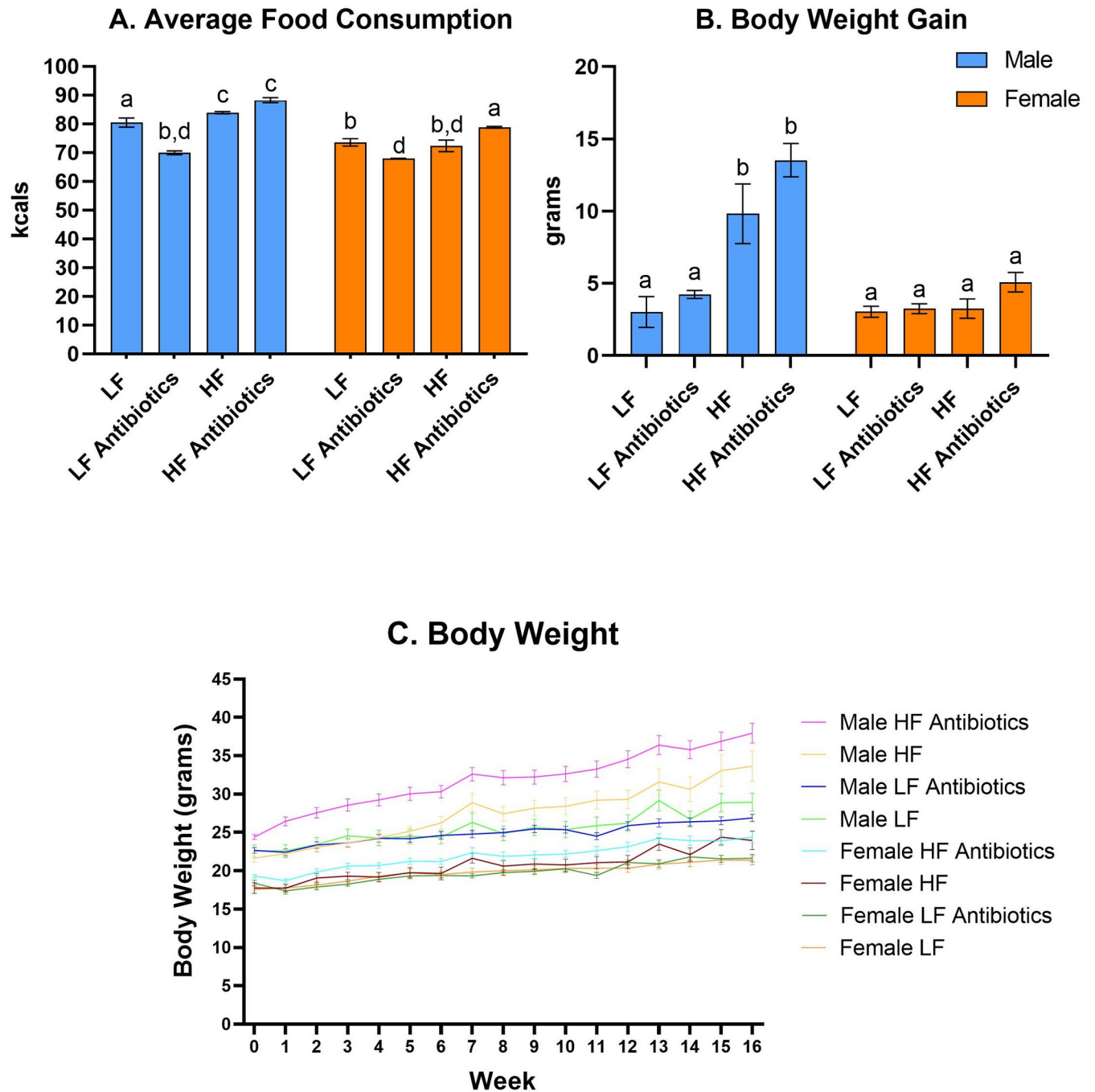
C. Body Weight

Fig 1. Average food consumption and body weight during the 16-week dietary study. (A) Average food consumption for the entire 16-week study. Different letters indicate groups that are significantly different (p<0.05). (B) HF-fed mice gained significantly more weight than LF-fed mice. Male HF and Male HF Antibiotics gained significantly more weight than all other groups. (C) Male HF Antibiotics reveal the highest body weight; Female LF and Female LF Antibiotics reveal the lowest body weight. Values shown are mean ± SEM.

https://doi.org/10.1371/journal.pone.0265850.g001

We determined statistically significant differences for fecal microbiome genera due to antibiotics, as well as sex and diet alone ([Table 1](#)). The HF diet significantly changed genera abundances for both sexes compared to the LF diet. For example, *Clostridium*, *Lachnoclostridium*, *Oscillospira*, *Sporobacter*, and *Tyzzerella* were increased to a similar extent for both male and

A. Shannon Diversity

B. Operational Taxonomic Unit

C. Faith's Phylogenetic Diversity
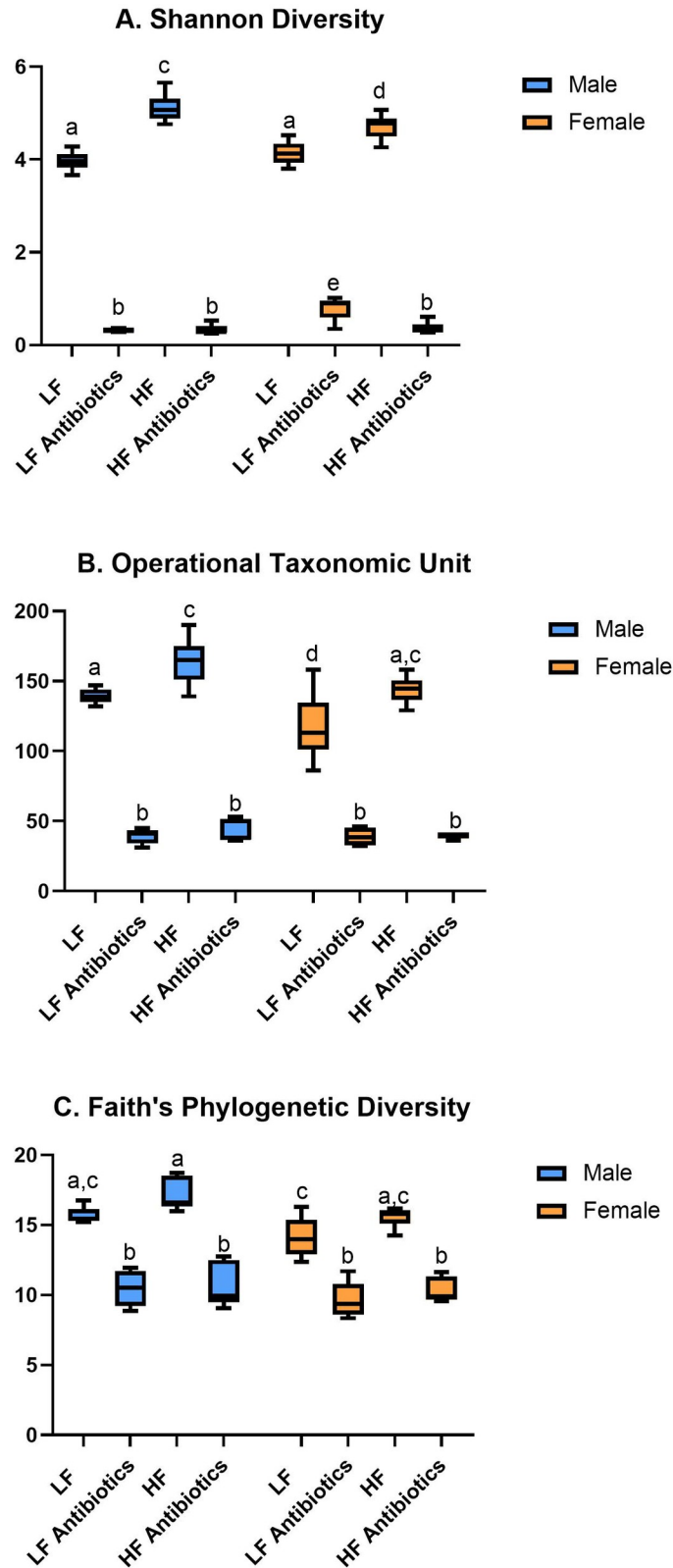
Fig 2. Fecal microbiome alpha diversity (n = 6/group). (A) There was a significant effect of treatment (p<0.0001) and a significant interaction effect (sex x treatment; p = 0.0002) for Shannon Diversity. (B) There was a significant effect of treatment (p<0.0001) and a significant effect of sex (p = 0.0021) on Operational Taxonomic Units. (C) There

was a significant effect of treatment (p<0.0001) and a significant effect of sex (p = 0.0026) on Faith's Phylogenetic Diversity.

female mice fed the HF diet compared to males and females fed the LF diet. *Allobaculum* and *Citrobacter* were decreased to a similar extent for male and female HF mice compared to male and female LF mice. On the other hand, *Lactobacillus* was significantly higher in Female LF mice compared to all other groups. *Turicibacter* and *Blautia* were significantly lower in Female HF mice compared to all other groups. Lastly, *Barnesiella* was significantly higher in Female HF mice compared to all other groups.

Microglial morphology characterization

FracLac and Skeleton analyses were performed to evaluate microgliosis. There was a significant sex x treatment interaction ($F_{(3,27)}$ = 15.02, p < 0.0001), significant effect of treatment ($F_{(3,27)}$ = 5.547, p = 0.0042), and significant effect of sex ($F_{(1,27)}$ = 7.073, p = 0.0130) for fractal analysis (Fig 6A). Female LF Antibiotics revealed significantly greater values for endpoint and branch length per soma compared to Female LF (p = 0.0002) and Male LF Antibiotics (p<0.0001). Interestingly, Male LF Antibiotics displayed decreased fractal analysis values compared to Male LF (p = 0.0432). The increased values for Female LF Antibiotics are indicative of resting microglia, with numerous, long processes.

There was a significant effect of treatment ($F_{(3,27)}$ = 5.633, p = 0.0039), sex ($F_{(1,27)}$ = 6.751, p = 0.0150) and a significant sex x treatment interaction ($F_{(3,27)}$ = 14.44, p < 0.0001) on branch length (Fig 6B), supporting the findings for fractal analysis: Female LF Antibiotics revealed the greatest branch length compared to the other groups. A significant sex x treatment interaction was also determined for cell complexity ($F_{(3, 27)}$ = 3.753, p = 0.0225; Fig 6C). There was a significant effect of treatment on cell shape ($F_{(3,27)}$ = 3.133, p = 0.0419; Fig 6D). Lastly, there was a significant effect of treatment ($F_{(3,27)}$ = 4.367, p = 0.0125) and a significant interaction effect ($F_{(3,27)}$ = 11.65, p < 0.0001) for summed endpoints (Fig 6F). Altogether, these data point to microglia in a resting-like state for Female LF Antibiotics and an activated-
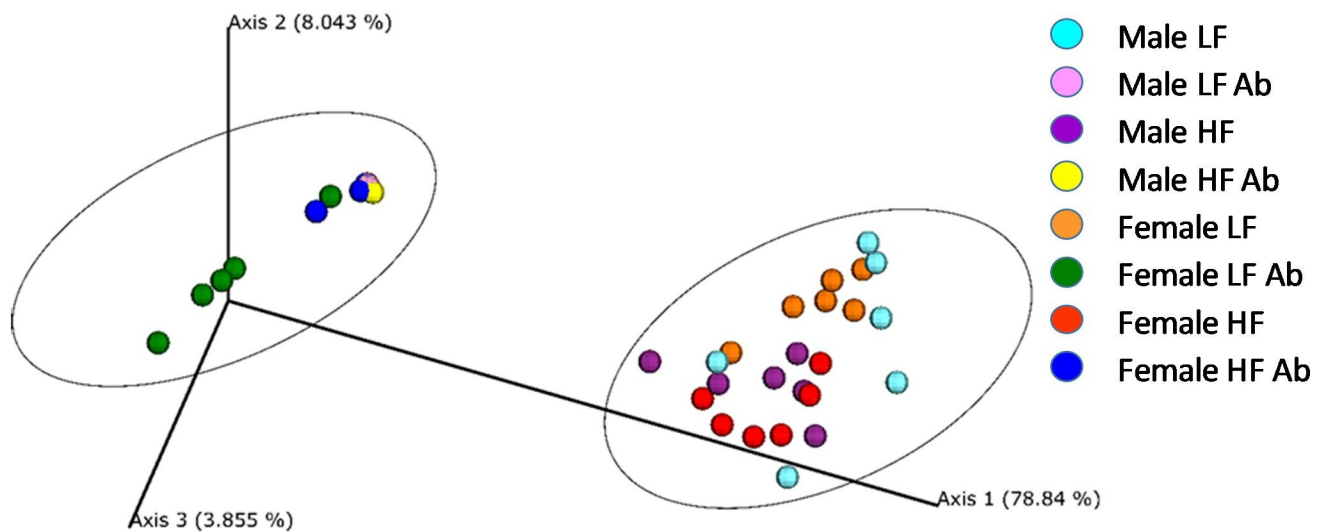
Fig 3. Principle coordinate plot of weighted UniFrac data (n = 6/group). The primary vector explains 78.8% of the variation between the groups. The first 3 vectors together exhibit 90.7% of the variation among the groups.
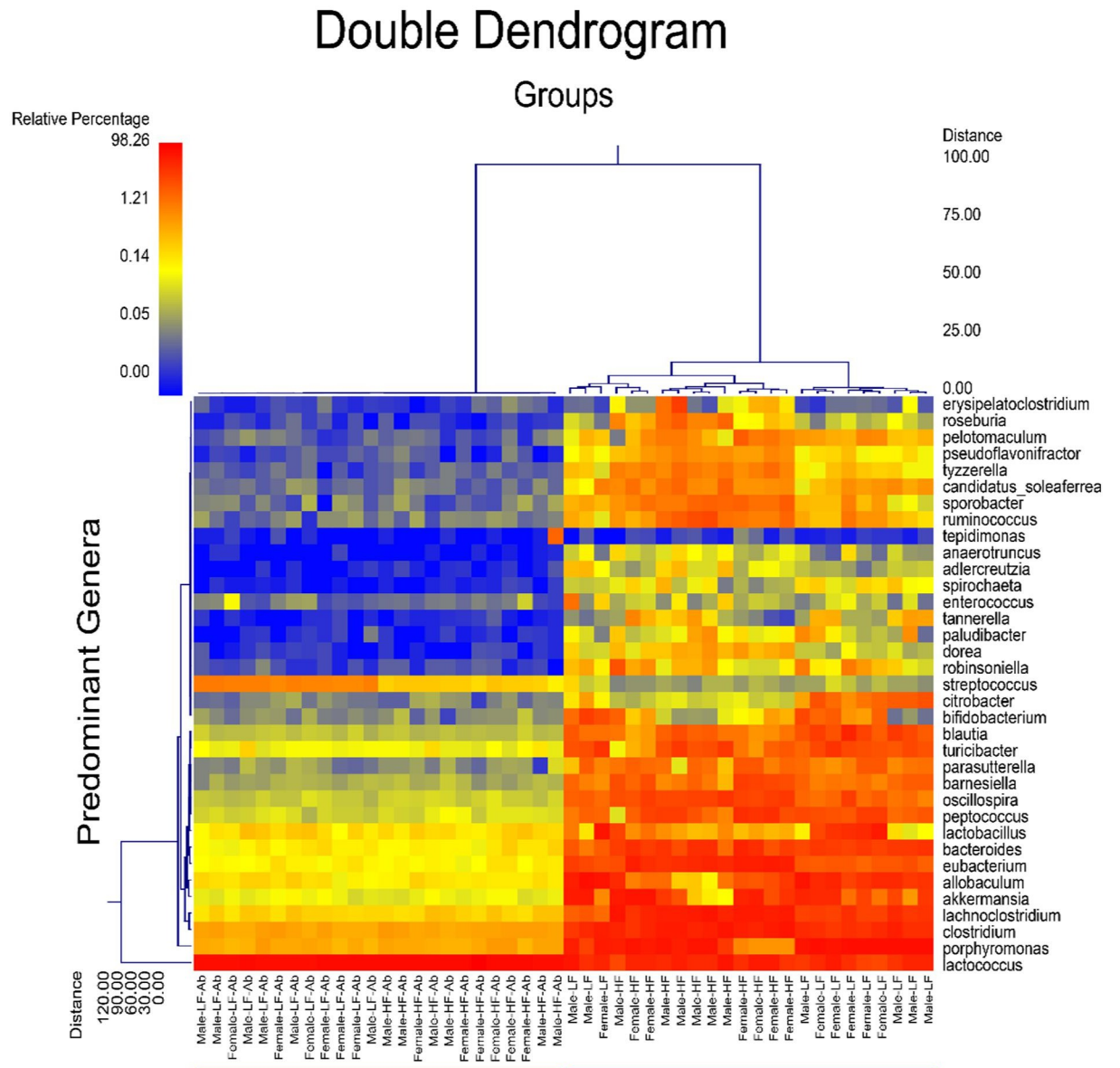
Fig 4. Dual hierarchical dendrogram (n = 6/group). To provide a visual overview combined with analysis, a dual hierarchal dendrogram was used to display the data for the predominant genera with clustering related to the different groups. Samples with more similar microbial populations were mathematically clustered closer together. The genera (consortium) were used for clustering. The samples with more similar consortium of genera cluster closer together with the length of connecting lines (top of heatmap) related to the similarity, shorter lines between two samples indicate closely-matched microbial consortium. The heatmap represents the relative percentages of each genus. The predominant genera are represented along the right Y-axis. The legend for the heatmap is provided in the upper left corner. The heat map and clustering reveals a significant effect of antibiotic treatment.

https://doi.org/10.1371/journal.pone.0265850.g004

like state for Male LF Antibiotics. Antibiotics did not significantly impact HF-fed mice, regardless of sex. However, Female HF Antibiotics did reveal more endpoints, greater branch length, and greater cell complexity compared to Female HF. Male HF Antibiotics displayed slightly greater endpoints, branch length, and complexity compared to Male HF. Representative micrographs of microglia taken at 100X are displayed in Fig 7.

Fractal analysis correlated with the Shannon Diversity index. Interestingly, there seems to be a positive and negative correlation, depending on which group is plotted. In Fig 8A, data
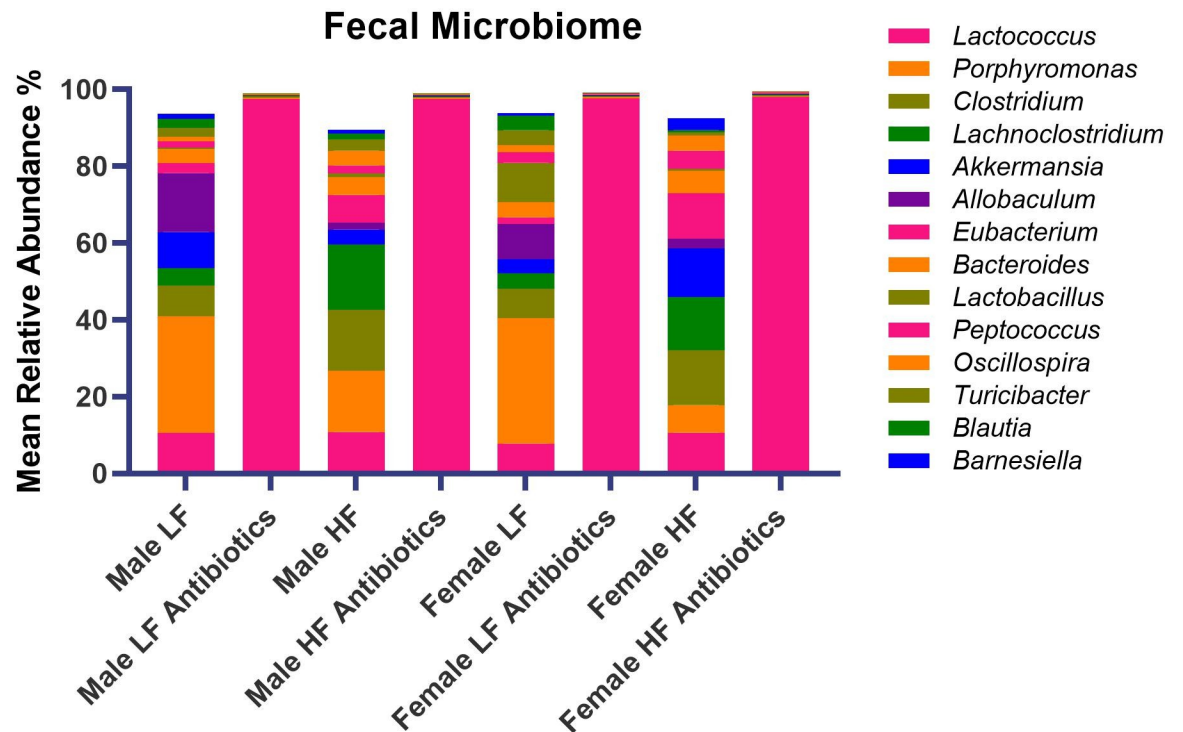
Fecal Microbiome

Fig 5. Genus-level relative abundances in the fecal microbiome (n = 6/group). Average relative abundance for the top 14 most abundant genera are displayed for each of the 8 experimental groups.

from all eight groups is presented. Antibiotic-treated groups revealed a low Shannon Diversity index and a positive correlation with Fractal Analysis. On the other hand, normal drinking water-treated groups revealed a higher Shannon Diversity index and a negative correlation with Fractal analysis. When analyzed separately, antibiotic-treated groups reveal a significant positive correlation (Spearman r = 0.5637; p = 0.0203; Fig 8B). Normal drinking water groups revealed a significant negative correlation (Spearman r = -0.5735; p = 0.0223; Fig 8C).

Astrocyte analysis

There was a significant treatment effect for GFAP densitometry (F(3,31) = 13.18, p<0.0001; Fig 9). Overall, Male and Female LF Antibiotics revealed decreased GFAP density compared to the other groups, reaching statistical significance in the Female LF Antibiotics group compared to the Female LF group (p = 0.0007). Representative micrographs of astrocytes taken at 10X in the CA1 region of the hippocampus are presented.

Discussion

Previous research has reported increased weight gain in male mice compared to female mice, despite being fed the same obesity-inducing diet [9, 10]. In this study, male mice gained significantly greater weight compared to female mice. Proposed explanations for this female resistance to weight gain include increased estrogen levels, lower levels of the pro-inflammatory cytokine IL-6, and increased levels of the short-chain fatty acid, butyrate (a gut metabolite) compared to male mice [13–16]. However, further research is needed to fully understand the mechanism by which resistance to diet-induced obesity occurs in female mice. Additionally, our study demonstrated that the Male HF Antibiotics group had the highest average weight

Table 1. Statistically significant differences in gut microbiome relative abundances.

Genus	Male LF vs. Male LF Antibiotics	Male HF vs. Male HF Antibiotics	Female LF vs. Female LF Antibiotics	Female HF vs. Female HF Antibiotics	Male LF vs. Male HF	Female LF vs. Female HF	Male LF vs. Female LF	Male HF vs. Female HF
Lactococcus	p = 0.0246	p = 0.0015	p = 0.0023	p = 0.0007				
Porphyromonas	p = 0.0003	p = 0.0133	p = 0.0002	p = 0.0373		p = 0.0043		
Clostridium	p = 0.0069	p = 0.0007	p = 0.0100	p = 0.0013	p = 0.0338	p = 0.0338		
Lachnoclostridium	p = 0.0320	p = 0.0010	p = 0.0078	p = 0.0002	p = 0.0029	p = 0.0062		
Akkermansia	p = 0.0008	p = 0.0141	p = 0.0209	p = 0.0003				
Allobaculum	p = 0.0028		p = 0.0003	p = 0.0100	p = 0.0019	p = 0.0412		
Eubacterium	p = 0.0061	p = 0.0021		p < 0.0001	p = 0.0455	p = 0.0002		
Bacteroides	p = 0.0039	p = 0.0020	p = 0.0069	p = 0.0014				
Lactobacillus		p = 0.0133	p = 0.0003	p = 0.0246		p = 0.0114	p < 0.0001	
Peptococcus	p = 0.0069		p = 0.0003	p = 0.0011				
Oscillospira	p = 0.0069	p = 0.0023	p = 0.0094	p = 0.0004	p = 0.0055	p = 0.0179		
Turicibacter	p = 0.0088	p = 0.0065	p = 0.0002	p = 0.0221		p = 0.0007		p = 0.0247
Blautia	p = 0.0005	p = 0.0036	p = 0.0015	p = 0.0198		p = 0.0004		p = 0.0455
Barnesiella	p = 0.0015		p = 0.0141	p < 0.0001		p = 0.0008		p = 0.0062
Parasutterella	p = 0.0094	p = 0.0106	p = 0.0011	p = 0.0005				
Bifidobacterium			p = 0.0004	p = 0.0150				
Ruminococcus	p = 0.0209	p < 0.0001	p = 0.0112	p = 0.0047	p = 0.0005			
Sporobacter	p = 0.0187	p = 0.0002	p = 0.0392	p = 0.0001	p = 0.0029	p = 0.0062		
Citrobacter	p = 0.0002	p = 0.0233	p = 0.0003	p = 0.0337	p = 0.0043	p = 0.0025		
Candidatus soleaferrea	p = 0.0233	p = 0.0007	p = 0.0074	p = 0.0004	p = 0.0019			
Tyzzerella	p = 0.0158	p = 0.0009	p = 0.0119	p = 0.0003	p = 0.0017	p = 0.0062		
Pelotomaculum	p = 0.0412	p = 0.0177	p = 0.0014	p < 0.0001				
Streptococcus	p = 0.0001	p = 0.0119	p = 0.0057	p = 0.0078				
Roseburia	p = 0.0073	p < 0.0001		p = 0.0004	p = 0.0007	p = 0.0128		
Pseudoflavonifractor	p = 0.0150	p = 0.0001	p = 0.0304	p = 0.0006	p = 0.0076			
Dorea	p = 0.0369	p < 0.0001	p = 0.0249	p = 0.0006	p = 0.0037	p = 0.0048		
Paludibacter	p = 0.0043	p = 0.0010	p = 0.0084	p = 0.0024				
Spirochaeta	p = 0.0013	p = 0.0049	p = 0.0001	p = 0.0439				
Adlercreutzia	p = 0.0012	p = 0.0019	p = 0.0045	p = 0.0058				

gain. This aligns with research that suggests an association between antibiotic usage and increased weight gain, with early antibiotic exposure resulting in the greatest amount of weight gain [51–53]. Furthermore, antibiotic usage is known to increase animal growth and weight and is a common practice for livestock farming [54]. Despite its known effect on animals, further research into prolonged antibiotic exposure and its relationship with adult human weight gain is needed, especially due to the rising use of antibiotics in modern society.

Caloric consumption for individual animals was calculated and recorded each week during the 16-week study. Since the animals were housed 2 to 4 in a cage, individual caloric consumption for each animal was calculated by dividing the total number of calories consumed for the entire cage by the number of mice within the cage. While this does present a limitation to our study as we did not accurately determine individual mouse caloric consumption, individual housing of mice was not preferred as it has been shown to significantly impact weight gain and food consumption [55]. Fortunately, all mice were able to remain in group-housing conditions throughout the entire study. Regardless of sex, antibiotic treatment lowered caloric intake for
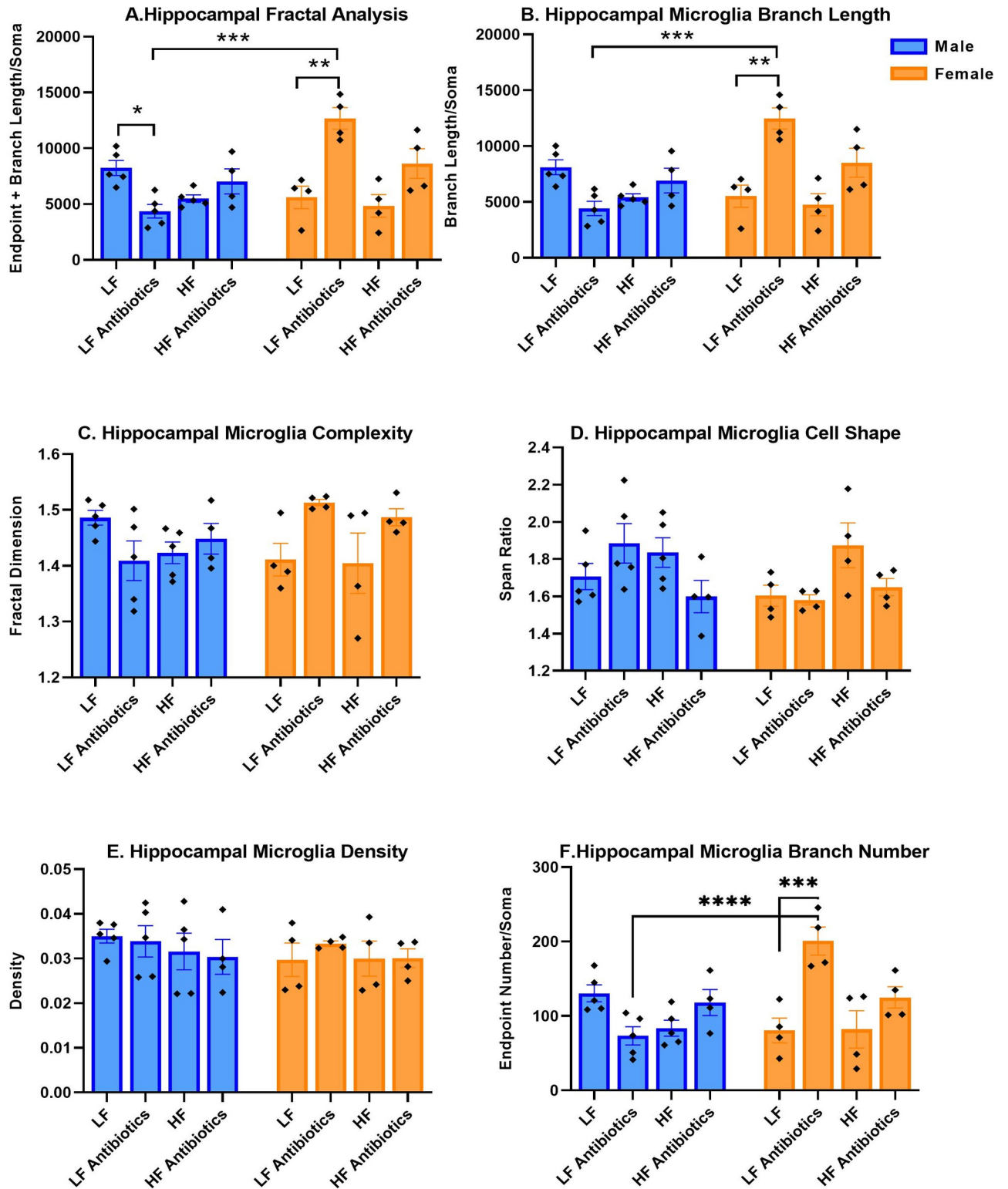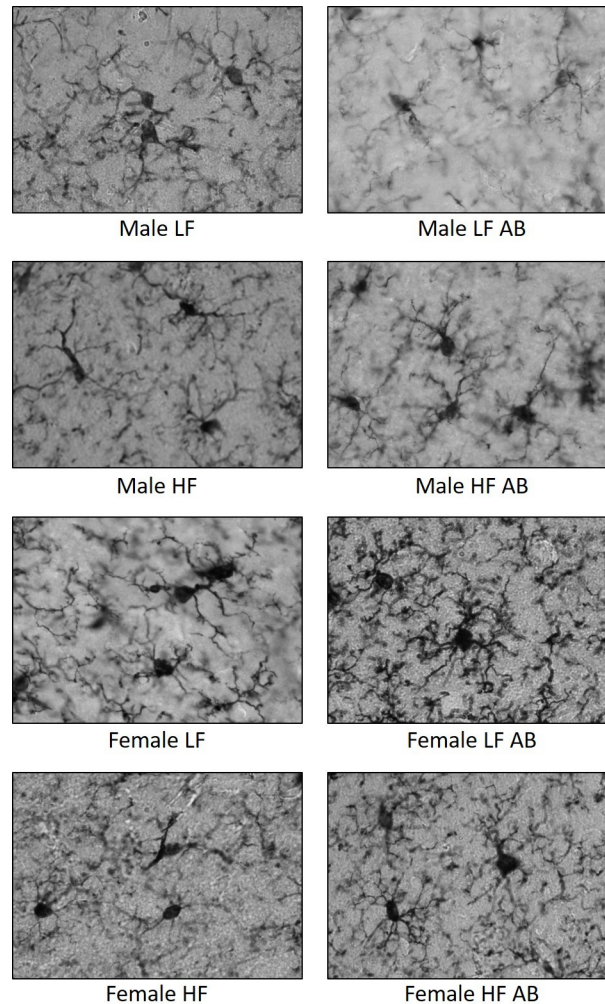
Fig 6. Microglial analysis (n = 4-5/group). The results for fractal analysis (A), branch length (B), cell complexity (C), cell shape (D), density (E), and summed endpoints (F) are shown. * p<0.05; *** p<0.001; **** p<0.0001.

https://doi.org/10.1371/journal.pone.0265850.g006

Fig 7. Representative micrographs of microglia. 100X images were collected for microglia labeled with the Iba-1 antibody.

LF groups and increased caloric intake for HF groups. Male HF and Male HF Antibiotics consumed, on average, significantly more calories than Female HF and Female HF Antibiotics, respectively. Male LF consumed significantly more calories than Female LF. However, there were no significant differences in caloric consumption between Male LF Antibiotics and Female LF Antibiotics.

Sex differences and treatment effects were also determined for the fecal microbiome. In a previous study, we reported genus-level differences due to sex and/or diet [9]. Interestingly, we determined different effects to fecal bacteria in our current study. For example, we previously determined significant differences due to sex for *Allobaculum*, *Peptococcus*, *Blautia*, *Ruminococcus*, *Pelotomaculum*, *Paludibacter*, and *Adlercreutzia* that we did not determine in the current study. In the current study, we determined that *Lactobacillus*, *Turicibacter*, *Blautia*, and *Barnesiella* were altered due to sex. The housing conditions, diet, and source for the mice were the same between studies. However, it has previously been shown that stochastic changes to the microbiome can occur despite controlling multiple variables including housing conditions, animal vendor, and diet [56]. We did determine some overlapping results between our previous and current study: *Allobaculum*, *Eubacterium*, and *Citrobacter* changed due to diet.
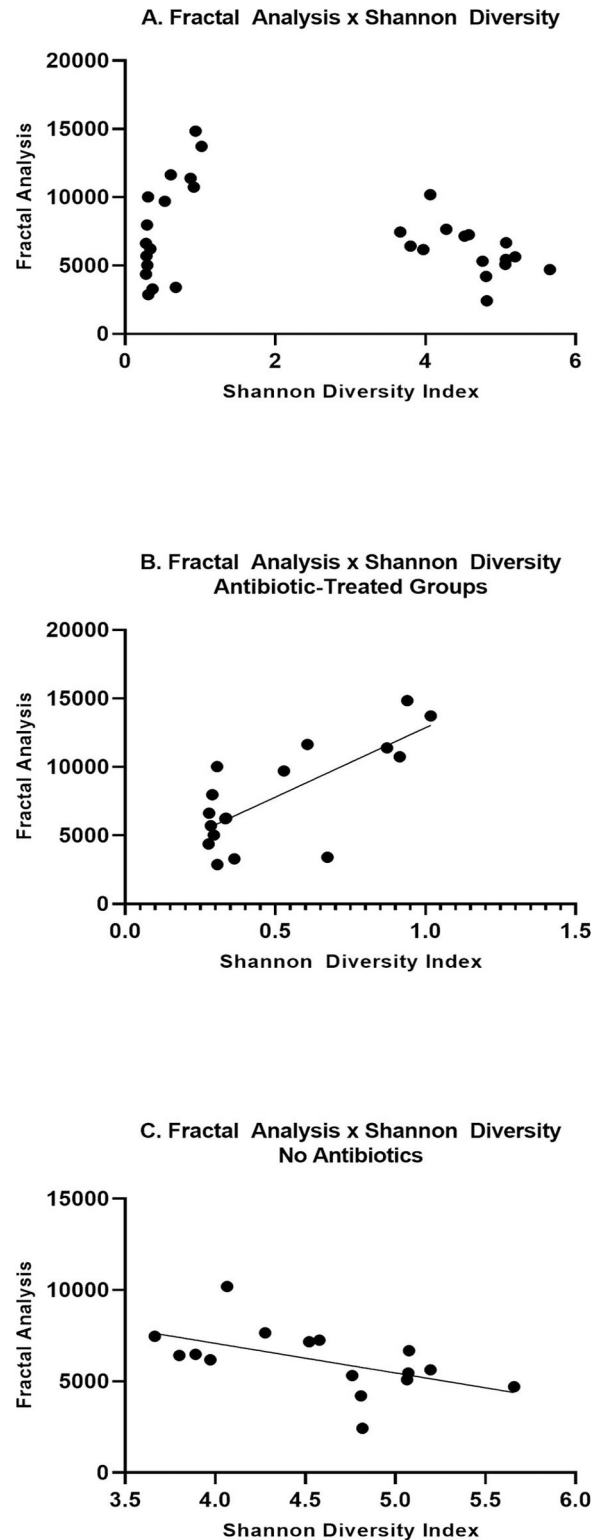
Fig 8. Correlations for fractal analysis and Shannon Diversity. (A) All groups are plotted, including results with low Shannon diversity for antibiotic-treated vs. higher Shannon diversity for mice that received normal drinking water. (B) A positive correlation (Spearman r = 0.5637; p = 0.0203) was determined for antibiotic-treated mice. (C) A negative correlation (Spearman r = -0.5735; p = 0.0223) was determined for normal drinking water mice.

https://doi.org/10.1371/journal.pone.0265850.g008
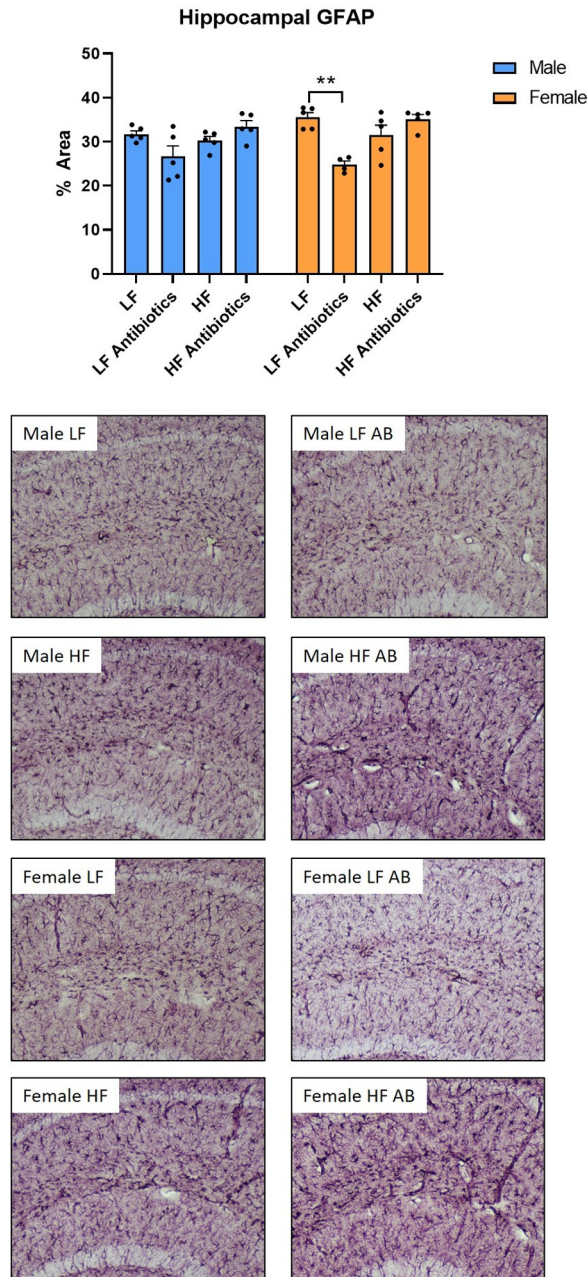
Fig 9. GFAP densitometry (n = 5/group). Female LF Antibiotics revealed a significant decrease in GFAP densitometry in the hippocampus compared to Female LF. ** p < 0.01. Representative micrographs of images taken at 10X following labeling with a GFAP antibody are presented.

Antibiotic-treated mice revealed a significant reduction in diversity as well as significant depletion of specific genera of bacteria. *Lactococcus* was the primary genus of bacteria present in antibiotic-treated mice, regardless of sex. For all bacteria shown in Fig 5, antibiotics decreased the abundance, except for *Lactococcus*, which was significantly greater in abundance compared to control animals given normal drinking water. It is possible that without competition from other genera of bacteria, *Lactococcus* could over-populate the microbiome. Interestingly, Female LF Antibiotics revealed significantly higher Shannon diversity compared to the other

antibiotic-treated groups. Female LF Antibiotics also lacked a significant change to *Eubacte-rium* and *Roseburia* abundance compared to Female LF, whereas all other groups indicated significant decreases in these genera when compared to their control counterparts. It is not likely that these differences fully account for the observed differences in neurogliosis, however it is possible that gut microbiome diversity contributes to altered glial health [57, 58]. We did determine that Shannon diversity correlated with fractal analysis (Frac Lac; Fig 8). Previous studies have shown that increased species richness within the gut microbiome is correlated with decreased microgliosis [57, 59].

Previous studies have also shown that males have greater amounts of microglial cells compared to females. However, females have a greater number of activated microglial cells [60]. In the present study, we characterized hippocampal microglial cell features using fractal analysis (branch length plus endpoints per soma), fractal dimension (cell complexity), circularity, density, and span ratio (cell shape) values. Activated microglial cells are characterized by decreased values for branch length plus endpoints, cell complexity (fractal dimension), and increased values for span ratio, circularity, and density. In contrast, extensive branching and greater cell complexity are indicative of resting microglial cells. We observed features of resting microglia for Female LF Antibiotics, including increased branch length, increased branch number, and increased cell complexity (not statistically significant). On the other hand, Male LF Antibiotics revealed a significantly lower value for fractal analysis compared to Male LF. This change could indicate more activated microglia for male LF-fed mice following antibiotics administration. We were surprised that antibiotic administration led to striking sex differences, and only in LF-fed mice.

In a recent study by Cordella et al., male mice fed a standard diet and administered gentamicin and vancomycin in drinking water supplemented with sugar revealed increased microglial density, but no change to morphology, in the hippocampus [61]. This study only focused on male mice and therefore, sex differences under the experimental parameters were not assessed. However, a lack of change to microglial morphology following antibiotic administration is in contrast to our findings. It is possible that since our low fat diet does not contain sucrose, it caused additional changes to microglia morphology, and possibly, their metabolism. We did not supplement the drinking water with sucrose. In a study by Zarrinpar et al., male mice were administered an antibiotic cocktail with the same antibiotics that we utilized, but also included the anti-fungal, amphotericin B. Both the control group and antibiotic-treatment group were fed a normal-chow diet (LabDiet 5001). They determined that antibiotic treatment improved glucose tolerance and insulin sensitivity [62], as also shown in previous studies [42, 63, 64]. It was further reported that antibiotic treatment increased levels of glucagon-like peptide 1 (GLP-1) as well as decreased the short chain fatty acid (SCFA), butyrate. Given increased energy demand in the colon due to higher levels of GLP-1 and the lack of butyrate as fuel, the gut could increase glucose utilization, in particular, via anaerobic glycolysis. This would result in cecal enterocytes utilizing higher levels of glucose, leading to overall changes to metabolic homeostasis throughout the body. In our study, the low fat diet did not deliver sucrose and we did not include any sucrose in the drinking water. The main source of carbohydrate for the diet was corn starch. While corn starch consists of glucose polymers, it is possible that there is a reduced capacity for breakdown of starch in the intestine following antibiotic administration and subsequently, decreased absorption of glucose. In a future experiment, we will need to evaluate blood glucose levels and insulin sensitivity. Interestingly, it has been proposed that glucose metabolism exerts transcriptional control over microglial activation [65–67]. Glucose is the primary fuel for microglia, as it is for neurons. Under inflammatory conditions, glucose transporter 1 (GLUT1) is upregulated in order for glucose uptake and glycolysis to increase in microglia. When glucose is unavailable, free fatty acids can be a secondary fuel for microglia

[68]. It is possible that in our study, the low-fat, no sucrose diet in addition to a depleted microbiome, resulted in a lack of fuel in the form of glucose, as well as the back-up fuel in the form of free fatty acids. This lack of fuel could have inhibited microglial activation in Female LF Antibiotics mice. We did not observe the same effect in male mice, which could be protected by their slightly higher adiposity. However, Male LF Antibiotics did not consume more calories than Female LF Antibiotics. It is also possible that baseline sex differences in glucose and lipid metabolism as well as gut microbiome composition impacted these results. In a recent study by Peng et al., both male and female C57Bl/6 mice were fed either a chow diet (Research Diets D12450B) or high fat diet (Research Diets D12451) and administered the same antibiotic cocktail as in our study. However, antibiotics were provided before diet administration and the chow diet animals were not included for antibiotic treatment. Their study reported increased weight gain, insulin resistance, and fasting blood glucose in male mice compared to female mice. Additionally, they determined sex differences in the fecal microbiome. For example, *Parabacteroides*, *Lactobacillus*, *and Bifidobacterium* were increased in female mice compared to male mice [69]. We also observed significantly higher levels of *Lactobacillus* for our Female LF mice, but this was significantly decreased following antibiotic treatment. Previous research has determined that some strains of *Lactobacillus* have anti-inflammatory effects [69, 70]. Peng et al. also observed decreased *Roseburia* in high fat-fed male mice, but it was increased in mice administered antibiotics. On the other hand, *Roseburia* was decreased in antibiotic-treated high fat-fed female mice. In our study, high fat diet treatment significantly increased *Roseburia* abundance for both sexes, but to a greater extent in male mice. Antibiotic treatment significantly decreased *Roseburia* abundance in both sexes and both diets. In the study by Peng et al., *Roseburia* was implicated in improved glucose metabolism and it was further discussed that *Roseburia* is a proposed probiotic that increases production of SCFAs [69]. The difference in abundance of this genus of bacteria between the two studies may be due to timing of antibiotic treatment; we included antibiotic treatment for 6 weeks following 10 weeks of diet as well as in conjunction with diet, while Peng et al. pre-treated with antibiotics for 4 weeks, stopped antibiotic treatment, and then started the high fat diet. We determined sex differences in fecal microbiome composition, which could result in altered metabolite production, inflammation, and overall metabolism.

Furthermore, metronidazole was included in our antibiotic cocktail. Metronidazole is an absorbable antibiotic that does cross the blood brain barrier (BBB), which could lead to differences in its direct effects on microglial activation. However, the extent to which metronidazole penetrates the BBB and the subsequent effect on microglia is not yet fully understood [50, 71]. Future experiments, including those investigating sex differences in response to metronidazole, should be conducted. Additionally, Female LF Antibiotics revealed decreased GFAP expression compared to Female LF. Male LF Antibiotics also revealed decreased GFAP expression compared to Male LF, but not to the same extent as females. Astrocytes are involved in numerous functions, from immune support to BBB support to metabolism. However, it is possible that the decrease in GFAP expression for LF-fed, antibiotic-administered mice is an indicator of decreased nutrient load and decreased metabolic activity. The LF diet is lower in fat, does not contain sucrose, and is lower in calories; and, the decreased bacterial load following antibiotics administration could further contribute to a decrease in nutrients due to altered microbial metabolism.

The limitations of our study include a lack of metabolic measurements, including fasting glucose, insulin sensitivity, and SCFA analysis, a lack of analysis for the contribution of metronidazole and its direct effects on the brain, and a lack of analysis of the gut-brain axis. Here, we focused on sex differences in the fecal microbiome and hippocampal microglia characterization. An alternative approach could include testing germ-free mice, however, changes to

microglial morphology have already been determined with the germ-free mouse model [43] and our goal was to deplete the microbiome short-term following exposure to the low fat or high fat diet.Next steps will require further investigation of metabolic parameters as well as directly probing the gut-brain axis in order to better understand its role. Nonetheless, we report sex differences in fecal microbiome composition as well as morphological differences in hippocampal morphology in response to diet and antibiotic treatment.

Conclusions

We report sex, diet, and antibiotic effects on weight gain, food consumption, and fecal microbiome composition. We further report significantly decreased microgliosis and astrogliosis in the hippocampus for Female LF Antibiotics compared to Female LF whereas Male LF Antibiotics revealed increased microgliosis compared to Male LF. We hypothesize this effect is due to reduced fuel and subsequently, reduced capacity for microglial activation in Female LF Antibiotics mice. This sex difference brings forward questions about sex differences in nutrient metabolism, gut microbiome composition, response to antibiotics, and neurogliosis.

Future studies investigating the direct contribution of diet and the direct contribution of antibiotics to neuroglial health are necessary. Furthermore, the pathway(s) along the gut-brain axis that modulate glial response, including their sex differences, are an essential next-step.

Author Contributions

Conceptualization: Linnea Ruth Freeman.

Data curation: Anju Saxena, Roberta R. M. Moran, Meghan R. Bullard, Emma O. Bondy, Matthew Foster Smith, Lainie Morris, Nicaella Fogle, Jagroop Singh, Brendan Jarvis, Tammy Ray, Juhi Saxena.

Formal analysis: Anju Saxena, Roberta R. M. Moran, Matthew Foster Smith, Lainie Morris, Jagroop Singh, Juhi Saxena, Linnea Ruth Freeman.

Funding acquisition: Linnea Ruth Freeman.

Investigation: Anju Saxena, Roberta R. M. Moran.

Project administration: Linnea Ruth Freeman.

Resources: Linnea Ruth Freeman.

Supervision: Linnea Ruth Freeman.

Validation: Linnea Ruth Freeman.

Writing – original draft: Anju Saxena, Roberta R. M. Moran, Matthew Foster Smith, Linnea Ruth Freeman.

Writing – review & editing: Linnea Ruth Freeman.

References

1. Wang Y, Beydoun MA, Min J, Xue H, Kaminsky LA, Cheskin LJ. Has the prevalence of overweight, obesity and central obesity levelled off in the United States? Trends, patterns, disparities, and future projections for the obesity epidemic. Int J Epidemiol. 2020; 49(3):810–23. https://doi.org/10.1093/ije/dyz273 PMID: 32016289

2. Fryar CD, Gu Q, Ogden CL. Anthropometric reference data for children and adults: United States, 2007–2010. Vital Health Stat 11. 2012(252):1–48. PMID: 25204692

3. Hales CM, Carroll MD, Fryar CD, Ogden CL. Prevalence of Obesity and Severe Obesity Among Adults: United States, 2017–2018. NCHS Data Brief. 2020(360):1–8. PMID: 32487284

4. Centers for Disease Control and Prevention [CDC]. Overweight and Obesity. [Internet]. 2020. Available from: https://www.cdc.gov/obesity/data/adult.html

5. Murphy EA, Velazquez KT, Herbert KM. Influence of high-fat diet on gut microbiota: a driving force for chronic disease risk. Curr Opin Clin Nutr Metab Care. 2015; 18(5):515–20. https://doi.org/10.1097/MCO.0000000000000209 PMID: 26154278

6. Yusuf S, Hawken S, Ounpuu S, Bautista L, Franzosi MG, Commerford P, et al. Obesity and the risk of myocardial infarction in 27,000 participants from 52 countries: a case-control study. Lancet. 2005; 366 (9497):1640–9. https://doi.org/10.1016/S0140-6736(05)67663-5 PMID: 16271645

7. Giugliano D, Ceriello A, Esposito K. The effects of diet on inflammation: emphasis on the metabolic syndrome. J Am Coll Cardiol. 2006; 48(4):677–85. https://doi.org/10.1016/j.jacc.2006.03.052 PMID: 16904534

8. Deshpande NG, Saxena J, Pesaresi TG, Carrell CD, Ashby GB, Liao MK, et al. High fat diet alters gut microbiota but not spatial working memory in early middle-aged Sprague Dawley rats. PLoS One. 2019; 14(5):e0217553. https://doi.org/10.1371/journal.pone.0217553 PMID: 31141574

9. Daly CM, Saxena J, Singh J, Bullard MR, Bondy EO, Saxena A, et al. Sex differences in response to a high fat, high sucrose diet in both the gut microbiome and hypothalamic astrocytes and microglia. Nutr Neurosci. 2020:1–15. https://doi.org/10.1080/1028415X.2020.1752996 PMID: 32297553

10. Dorfman MD, Krull JE, Douglass JD, Fasnacht R, Lara-Lince F, Meek TH, et al. Sex differences in microglial CX3CR1 signalling determine obesity susceptibility in mice. Nat Commun. 2017; 8:14556. https://doi.org/10.1038/ncomms14556 PMID: 28223698

11. Thaler JP, Yi CX, Schur EA, Guyenet SJ, Hwang BH, Dietrich MO, et al. Obesity is associated with hypothalamic injury in rodents and humans. J Clin Invest. 2012; 122(1):153–62. https://doi.org/10.1172/JCI59660 PMID: 22201683

12. Yang Y, Smith DL Jr, Keating KD, Allison DB, Nagy TR. Variations in body weight, food intake and body composition after long-term high-fat diet feeding in C57BL/6J mice. Obesity (Silver Spring). 2014; 22 (10):2147–55. https://doi.org/10.1002/oby.20811 PMID: 24942674

13. Pettersson US, Walden TB, Carlsson PO, Jansson L, Phillipson M. Female mice are protected against high-fat diet induced metabolic syndrome and increase the regulatory T cell population in adipose tissue. PLoS One. 2012; 7(9):e46057. https://doi.org/10.1371/journal.pone.0046057 PMID: 23049932

14. Asarian L, Geary N. Cyclic estradiol treatment normalizes body weight and restores physiological patterns of spontaneous feeding and sexual receptivity in ovariectomized rats. Horm Behav. 2002; 42 (4):461–71. https://doi.org/10.1006/hbeh.2002.1835 PMID: 12488112

15. Popko K, Gorska E, Stelmaszczyk-Emmel A, Plywaczewski R, Stoklosa A, Gorecka D, et al. Proinflammatory cytokines Il-6 and TNF-alpha and the development of inflammation in obese subjects. Eur J Med Res. 2010; 15 Suppl 2:120–2.

16. Zhuang P, Shou Q, Lu Y, Wang G, Qiu J, Wang J, et al. Arachidonic acid sex-dependently affects obesity through linking gut microbiota-driven inflammation to hypothalamus-adipose-liver axis. Biochim Biophys Acta Mol Basis Dis. 2017; 1863(11):2715–26. https://doi.org/10.1016/j.bbadis.2017.07.003 PMID: 28711599

17. Turnbaugh PJ, Backhed F, Fulton L, Gordon JI. Diet-induced obesity is linked to marked but reversible alterations in the mouse distal gut microbiome. Cell Host Microbe. 2008; 3(4):213–23. https://doi.org/10.1016/j.chom.2008.02.015 PMID: 18407065

18. Ley RE, Backhed F, Turnbaugh P, Lozupone CA, Knight RD, Gordon JI. Obesity alters gut microbial ecology. Proc Natl Acad Sci U S A. 2005; 102(31):11070–5. https://doi.org/10.1073/pnas.0504978102 PMID: 16033867

19. Turnbaugh PJ, Ley RE, Mahowald MA, Magrini V, Mardis ER, Gordon JI. An obesity-associated gut microbiome with increased capacity for energy harvest. Nature. 2006; 444(7122):1027–31. https://doi.org/10.1038/nature05414 PMID: 17183312

20. Cani PD, Amar J, Iglesias MA, Poggi M, Knauf C, Bastelica D, et al. Metabolic endotoxemia initiates obesity and insulin resistance. Diabetes. 2007; 56(7):1761–72. https://doi.org/10.2337/db06-1491 PMID: 17456850

21. Noh H, Jeon J, Seo H. Systemic injection of LPS induces region-specific neuroinflammation and mitochondrial dysfunction in normal mouse brain. Neurochem Int. 2014; 69:35–40. https://doi.org/10.1016/j.neuint.2014.02.008 PMID: 24607701

22. Braniste V, Al-Asmakh M, Kowal C, Anuar F, Abbaspour A, Toth M, et al. The gut microbiota influences blood-brain barrier permeability in mice. Sci Transl Med. 2014; 6(263):263ra158. https://doi.org/10.1126/scitranslmed.3009759 PMID: 25411471

23. Lin HV, Frassetto A, Kowalik EJ Jr, Nawrocki AR, Lu MM, Kosinski JR, et al. Butyrate and propionate protect against diet-induced obesity and regulate gut hormones via free fatty acid receptor 3-

independent mechanisms. PLoS One. 2012; 7(4):e35240. https://doi.org/10.1371/journal.pone.0035240 PMID: 22506074

24. Robb JL, Morrissey NA, Weightman Potter PG, Smithers HE, Beall C, Ellacott KLJ. Immunometabolic Changes in Glia—A Potential Role in the Pathophysiology of Obesity and Diabetes. Neuroscience. 2020; 447:167–81. https://doi.org/10.1016/j.neuroscience.2019.10.021 PMID: 31765625

25. Valdearcos M, Robblee MM, Benjamin DI, Nomura DK, Xu AW, Koliwad SK. Microglia dictate the impact of saturated fat consumption on hypothalamic inflammation and neuronal function. Cell Rep. 2014; 9(6):2124–38. https://doi.org/10.1016/j.celrep.2014.11.018 PMID: 25497089

26. Gzielo K, Kielbinski M, Ploszaj J, Janeczko K, Gazdzinski SP, Setkowicz Z. Long-Term Consumption of High-Fat Diet in Rats: Effects on Microglial and Astrocytic Morphology and Neuronal Nitric Oxide Synthase Expression. Cell Mol Neurobiol. 2017; 37(5):783–9. https://doi.org/10.1007/s10571-016-0417-5 PMID: 27541371

27. Lainez NM, Jonak CR, Nair MG, Ethell IM, Wilson EH, Carson MJ, et al. Diet-Induced Obesity Elicits Macrophage Infiltration and Reduction in Spine Density in the Hypothalami of Male but Not Female Mice. Front Immunol. 2018; 9:1992. https://doi.org/10.3389/fimmu.2018.01992 PMID: 30254630

28. Dubbelaar ML, Kracht L, Eggen BJL, Boddeke E. The Kaleidoscope of Microglial Phenotypes. Front Immunol. 2018; 9:1753. https://doi.org/10.3389/fimmu.2018.01753 PMID: 30108586

29. Young K, Morrison H. Quantifying Microglia Morphology from Photomicrographs of Immunohistochemistry Prepared Tissue Using ImageJ. J Vis Exp. 2018(136). https://doi.org/10.3791/57648 PMID: 29939190

30. Buckman LB, Thompson MM, Moreno HN, Ellacott KL. Regional astrogliosis in the mouse hypothalamus in response to obesity. J Comp Neurol. 2013; 521(6):1322–33. https://doi.org/10.1002/cne.23233 PMID: 23047490

31. Wang DD, Bordey A. The astrocyte odyssey. Prog Neurobiol. 2008; 86(4):342–67. https://doi.org/10.1016/j.pneurobio.2008.09.015 PMID: 18948166

32. Francis HM, Stevenson RJ. Higher reported saturated fat and refined sugar intake is associated with reduced hippocampal-dependent memory and sensitivity to interoceptive signals. Behav Neurosci. 2011; 125(6):943–55. https://doi.org/10.1037/a0025998 PMID: 22023100

33. Cournot M, Marquie JC, Ansiau D, Martinaud C, Fonds H, Ferrieres J, et al. Relation between body mass index and cognitive function in healthy middle-aged men and women. Neurology. 2006; 67 (7):1208–14. https://doi.org/10.1212/01.wnl.0000238082.13860.50 PMID: 17030754

34. Valladolid-Acebes I, Fole A, Martin M, Morales L, Cano MV, Ruiz-Gayo M, et al. Spatial memory impairment and changes in hippocampal morphology are triggered by high-fat diets in adolescent mice. Is there a role of leptin? Neurobiol Learn Mem. 2013; 106:18–25. https://doi.org/10.1016/j.nlm.2013.06.012 PMID: 23820496

35. Hao S, Dey A, Yu X, Stranahan AM. Dietary obesity reversibly induces synaptic stripping by microglia and impairs hippocampal plasticity. Brain Behav Immun. 2016; 51:230–9. https://doi.org/10.1016/j.bbi.2015.08.023 PMID: 26336035

36. Molteni R, Barnard RJ, Ying Z, Roberts CK, Gomez-Pinilla F. A high-fat, refined sugar diet reduces hippocampal brain-derived neurotrophic factor, neuronal plasticity, and learning. Neuroscience. 2002; 112 (4):803–14. https://doi.org/10.1016/s0306-4522(02)00123-9 PMID: 12088740

37. Cope EC, LaMarca EA, Monari PK, Olson LB, Martinez S, Zych AD, et al. Microglia Play an Active Role in Obesity-Associated Cognitive Decline. J Neurosci. 2018; 38(41):8889–904. https://doi.org/10.1523/JNEUROSCI.0789-18.2018 PMID: 30201764

38. Thirumangalakudi L, Prakasam A, Zhang R, Bimonte-Nelson H, Sambamurti K, Kindy MS, et al. High cholesterol-induced neuroinflammation and amyloid precursor protein processing correlate with loss of working memory in mice. J Neurochem. 2008; 106(1):475–85. https://doi.org/10.1111/j.1471-4159.2008.05415.x PMID: 18410513

39. Wake H, Moorhouse AJ, Jinno S, Kohsaka S, Nabekura J. Resting microglia directly monitor the functional state of synapses in vivo and determine the fate of ischemic terminals. J Neurosci. 2009; 29 (13):3974–80. https://doi.org/10.1523/JNEUROSCI.4363-08.2009 PMID: 19339593

40. Rakoff-Nahoum S, Paglino J, Eslami-Varzaneh F, Edberg S, Medzhitov R. Recognition of commensal microflora by toll-like receptors is required for intestinal homeostasis. Cell. 2004; 118(2):229–41. https://doi.org/10.1016/j.cell.2004.07.002 PMID: 15260992

41. Greer RL, Dong X, Moraes AC, Zielke RA, Fernandes GR, Peremyslova E, et al. Akkermansia muciniphila mediates negative effects of IFNgamma on glucose metabolism. Nat Commun. 2016; 7:13329. https://doi.org/10.1038/ncomms13329 PMID: 27841267

42. Rodrigues RR, Greer RL, Dong X, KN DS, Gurung M, Wu JY, et al. Antibiotic-Induced Alterations in Gut Microbiota Are Associated with Changes in Glucose Metabolism in Healthy Mice. Front Microbiol. 2017; 8:2306. https://doi.org/10.3389/fmicb.2017.02306 PMID: 29213261

43. Dowd SE, Sun Y, Secor PR, Rhoads DD, Wolcott BM, James GA, et al. Survey of bacterial diversity in chronic wounds using pyrosequencing, DGGE, and full ribosome shotgun sequencing. BMC Microbiol. 2008; 8:43. https://doi.org/10.1186/1471-2180-8-43 PMID: 18325110

44. Dowd SE, Callaway TR, Wolcott RD, Sun Y, McKeehan T, Hagevoort RG, et al. Evaluation of the bacterial diversity in the feces of cattle using 16S rDNA bacterial tag-encoded FLX amplicon pyrosequencing (bTEFAP). BMC Microbiol. 2008; 8:125. https://doi.org/10.1186/1471-2180-8-125 PMID: 18652685

45. Eren AM, Zozaya M, Taylor CM, Dowd SE, Martin DH, Ferris MJ. Exploring the diversity of Gardnerella vaginalis in the genitourinary tract microbiota of monogamous couples through subtle nucleotide variation. PLoS One. 2011; 6(10):e26732. https://doi.org/10.1371/journal.pone.0026732 PMID: 22046340

46. Swanson KS, Dowd SE, Suchodolski JS, Middelbos IS, Vester BM, Barry KA, et al. Phylogenetic and gene-centric metagenomics of the canine intestinal microbiome reveals similarities with humans and mice. ISME J. 2011; 5(4):639–49. https://doi.org/10.1038/ismej.2010.162 PMID: 20962874

47. Bolyen E, Rideout JR, Dillon MR, Bokulich NA, Abnet CC, Al-Ghalith GA, et al. Author Correction: Reproducible, interactive, scalable and extensible microbiome data science using QIIME 2. Nat Biotechnol. 2019; 37(9):1091. https://doi.org/10.1038/s41587-019-0252-6 PMID: 31399723

48. Freeman LR, Haley-Zitlin V, Stevens C, Granholm AC. Diet-induced effects on neuronal and glial elements in the middle-aged rat hippocampus. Nutr Neurosci. 2011; 14(1):32–44. https://doi.org/10.1179/174313211X12966635733358 PMID: 21535919

49. Morrison H, Young K, Qureshi M, Rowe RK, Lifshitz J. Quantitative microglia analyses reveal diverse morphologic responses in the rat cortex after diffuse brain injury. Sci Rep. 2017; 7(1):13211. https://doi.org/10.1038/s41598-017-13581-z PMID: 29038483

50. Erny D, Hrabe de Angelis AL, Prinz M. Communicating systems in the body: how microbiota and microglia cooperate. Immunology. 2017; 150(1):7–15. https://doi.org/10.1111/imm.12645 PMID: 27392533

51. Blaser MJ. Antibiotic use and its consequences for the normal microbiome. Science. 2016; 352 (6285):544–5. https://doi.org/10.1126/science.aad9358 PMID: 27126037

52. Cho I, Yamanishi S, Cox L, Methe BA, Zavadil J, Li K, et al. Antibiotics in early life alter the murine colonic microbiome and adiposity. Nature. 2012; 488(7413):621–6. https://doi.org/10.1038/nature11400 PMID: 22914093

53. Esposito S. Early Antibiotic Exposure and Childhood Weight Gain. JAMA. 2016; 316(5):541. https://doi.org/10.1001/jama.2016.7300 PMID: 27483072

54. Zimmerman DR. Role of Subtherapeutic levels of antimicrobials in pig production. J Anim Sci. 1986; 62 (3):6–16.

55. Robertson KL, Rowland NE. Effect of two types of environmental enrichment for singly housed mice on food intake and weight gain. Lab Anim (NY). 2005; 34(9):29–32. https://doi.org/10.1038/laban1005-29 PMID: 16195735

56. Fan TJ, Tchaptchet SY, Arsene D, Mishima Y, Liu B, Sartor RB, et al. Environmental Factors Modify the Severity of Acute DSS Colitis in Caspase-11-Deficient Mice. Inflamm Bowel Dis. 2018; 24(11):2394–403. https://doi.org/10.1093/ibd/izy244 PMID: 30312415

57. Erny D, Prinz M. How microbiota shape microglial phenotypes and epigenetics. Glia. 2020; 68(8):1655–72. https://doi.org/10.1002/glia.23822 PMID: 32181523

58. Mossad O, Erny D. The microbiota-microglia axis in central nervous system disorders. Brain Pathol. 2020; 30(6):1159–77. https://doi.org/10.1111/bpa.12908 PMID: 33073887

59. Wang Y, Wang Z, Wang Y, Li F, Jia J, Song X, et al. The Gut-Microglia Connection: Implications for Central Nervous System Diseases. Front Immunol. 2018; 9:2325. https://doi.org/10.3389/fimmu.2018.02325 PMID: 30344525

60. Schwarz JM, Sholar PW, Bilbo SD. Sex differences in microglial colonization of the developing rat brain. J Neurochem. 2012; 120(6):948–63. https://doi.org/10.1111/j.1471-4159.2011.07630.x PMID: 22182318

61. Cordella F, Sanchini C, Rosito M, Ferrucci L, Pediconi N, Cortese B, et al. Antibiotics Treatment Modulates Microglia-Synapses Interaction. Cells. 2021; 10(10). https://doi.org/10.3390/cells10102648 PMID: 34685628

62. Zarrinpar A, Chaix A, Xu ZZ, Chang MW, Marotz CA, Saghatelian A, et al. Antibiotic-induced microbiome depletion alters metabolic homeostasis by affecting gut signaling and colonic metabolism. Nat Commun. 2018; 9(1):2872. https://doi.org/10.1038/s41467-018-05336-9 PMID: 30030441

63. Chou CJ, Membrez M, Blancher F. Gut decontamination with norfloxacin and ampicillin enhances insulin sensitivity in mice. Nestle Nutr Workshop Ser Pediatr Program. 2008; 62:127–37; discussion 37–40. https://doi.org/10.1159/000146256 PMID: 18626197

64. Suarez-Zamorano N, Fabbiano S, Chevalier C, Stojanovic O, Colin DJ, Stevanovic A, et al. Microbiota depletion promotes browning of white adipose tissue and reduces obesity. Nat Med. 2015; 21 (12):1497–501. https://doi.org/10.1038/nm.3994 PMID: 26569380

65. Bernhart E, Kollroser M, Rechberger G, Reicher H, Heinemann A, Schratl P, et al. Lysophosphatidic acid receptor activation affects the C13NJ microglia cell line proteome leading to alterations in glycolysis, motility, and cytoskeletal architecture. Proteomics. 2010; 10(1):141–58. https://doi.org/10.1002/pmic.200900195 PMID: 19899077

66. Chenais B, Morjani H, Drapier JC. Impact of endogenous nitric oxide on microglial cell energy metabolism and labile iron pool. J Neurochem. 2002; 81(3):615–23. https://doi.org/10.1046/j.1471-4159.2002.00864.x PMID: 12065670

67. Won SJ, Kim JH, Yoo BH, Sohn M, Kauppinen TM, Park MS, et al. Prevention of hypoglycemia-induced neuronal death by minocycline. J Neuroinflammation. 2012; 9:225. https://doi.org/10.1186/1742-2094-9-225 PMID: 22998689

68. Lauro C, Limatola C. Metabolic Reprograming of Microglia in the Regulation of the Innate Inflammatory Response. Front Immunol. 2020; 11:493. https://doi.org/10.3389/fimmu.2020.00493 PMID: 32265936

69. Peng C, Xu X, Li Y, Li X, Yang X, Chen H, et al. Sex-specific association between the gut microbiome and high-fat diet-induced metabolic disorders in mice. Biol Sex Differ. 2020; 11(1):5. https://doi.org/10.1186/s13293-020-0281-3 PMID: 31959230

70. Sanders ME, Merenstein DJ, Reid G, Gibson GR, Rastall RA. Probiotics and prebiotics in intestinal health and disease: from biology to the clinic. Nat Rev Gastroenterol Hepatol. 2019; 16(10):605–16. https://doi.org/10.1038/s41575-019-0173-3 PMID: 31296969

71. Nau R, Sorgel F, Eiffert H. Penetration of drugs through the blood-cerebrospinal fluid/blood-brain barrier for treatment of central nervous system infections. Clin Microbiol Rev. 2010; 23(4):858–83. https://doi.org/10.1128/CMR.00007-10 PMID: 20930076